**Solid Freeform Fabrication 2024: Proceedings of the 35th Annual International Solid Freeform Fabrication Symposium – An Additive Manufacturing Conference
Reviewed Paper**

Process Development and Control for Sensor-Informed Hybrid-Additive Manufacturing

Dan Davie[1], Louis Masters[1], Matthew Shuttleworth[1], Jaemin Lee[1], Robert Kay[1]

[1]School of Mechanical Engineering, University of Leeds

Abstract

Hybrid-Additive Manufacturing (hybrid-AM) systems enable production of high-quality components by leveraging the advantages of multiple distinct process in a single manufacturing platform. However, novel process combinations create challenges for machine control due to the lack of machine-agnostic hybrid manufacturing software. This work presents improvements to a hybrid-AM platform for technical ceramics, incorporating multi-material extrusion (polymer filament and ceramic paste), infra-red drying, green machining, and multi-modal sensing. A bespoke software package was created to facilitate control of the distinct technologies and sensing operations using a single production file. Sensor data is used for process calibration and dynamic process parameter adjustment, increasing the systems intelligence. For example, layer height measurements using a laser profilometer are used to tune the paste extrusion parameters. This enables the integrated fabrication of ceramic components with ~ 0.1 mm precision, complex geometries and near theoretical density, creating new manufacturing opportunities in the technical ceramics market.

1. Introduction

Manufacturing technologies possess a distinct combination of advantages and disadvantages when used in isolation. Hybrid Manufacturing methods combine technologies into a single platform in a configuration that leverages the advantages of each [1,2]. Additionally, sensors can be used to monitor the build process in-situ. This can help the user to understand the effect of certain parameters on build quality, or could be used to dynamically adjust the parameters, enabling closed-loop manufacturing [3]. This approach has vast potential that is currently limited by the available hardware and corresponding software, yet limited literature exists surrounding the development of machine-agnostic software for control of hybrid-AM systems. This work details the developments and key aspects of a hybrid manufacturing platform and process for technical ceramic materials – including the hardware configuration, process flow, and CAD to control software pipeline. The scale up of advanced technologies such as this will be instrumental in bringing next-generation functional products to market, especially in high-value, heavily regulated industries such as aerospace or medical engineering.

2.1. Ceramic Hybrid Additive Manufacturing Platform

The Ceramic Hybrid Additive Manufacturing Platform (CHAMP, see figure 1) uses a hybrid process, combining multiple process operations to overcome challenges with existing ceramic AM methods [2]. This process has evolved significantly since it's conception. The following section introduces the hybrid approach and outlines the design rationale behind the implementation of key features and process developments.

- **Density** – AM technologies were typically designed around polymers and metals and have since been adapted to incorporate ceramic materials, once the pre- (material formulation) and post- (thermal) processing operations are considered, it becomes challenging and time consuming to achieve high density components [4,5]. Ceramic paste extrusion instead adapts the processing hardware to be suitable for conventional feedstock materials using water to enable flow.
- **Extrusion consistency** – the paste extrusion process is challenging to control. Pneumatic extrusion is force controlled and the volume of material dispensed is dependent on the viscosity of the material [6]. Mechanical actuation is velocity controlled and enables volumetric extrusion [7]. However, if the control volume (between actuator and nozzle tip) is large, there is a lag between actuation and extrusion which is a problem for a this stop-start process. An auger screw is used as a friction valve to control the extrusion start and stop.

1) 3 axis motion platform
2) Heated build plate
3) Polymer extruder
4) Ceramic paste extruder
5) Infra-red heat lamp
6) Green machining spindle
7) In-situ monitoring suite

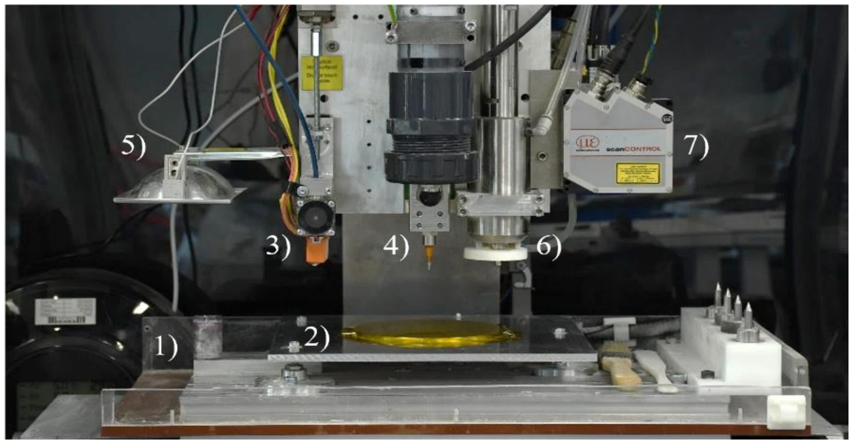

Figure 1 shows the ceramic hybrid additive manufacturing platform (CHAMP). Combining multiple distinct technologies in a single platform to leverage the advantages of each.

- **Resolution** – ceramic paste extrusion is a relatively low-resolution process as resolution and surface finish are inherently coupled to nozzle size and layer thickness [8].t Additionally, post-shaping drying of ceramic bodies causes shrinkage by the removal of water content, affecting the dimensional accuracy. Infra-red drying is used to enable green machining (subtractive manufacturing, SM) and preclude post-shaping drying shrinkage. Green machining is then used as a finishing operation to decouple the accuracy/resolution from the paste extrusion process.
- **Material formulation** – paste materials with suitable properties for extrusion require the material to be shear thinning and viscoelastic, developing a yield stress once extruded [9]. This can be achieved using additives to tailor the interparticle forces, which, can be challenging, especially with uncharacterised ceramic compositions. Interlayer drying accelerates the development of a yield stress in printed layers, decoupling the buildability from the rheological behaviour.
- **Durability** – green state ceramics possess a fraction of the strength of their sintered counterparts [10]. Furthermore, in the current process they must be sufficiently well attached to the substrate to be built and machined, and post-production removal can be challenging, see figure 2a. In CHAMP, ceramic parts are built on top of a polymer raft, deposited by a standard FFF nozzle, which adheres to a polyetherimide build surface, heated to 60ºC. As the build surface cools the raft detaches and can be used to handle the part. The raft also protects the build surface during machining operations and can either be removed from the part prior to, or burnt off during, sintering.
- **Machining Forces** – Typically, during subtractive manufacturing operations, the workpiece is rigidly held to the machine using a clamp or vice. In this case, the part is only held by adhesion to the build plate and can easily detach if the cutting forces are too high, see figure 2b. Subtractive toolpath parameters are chosen that reduce machining forces, e.g., by reducing the depth of cut.
- **Nozzle blockages –** during non-print operations, the paste material can dry out in the nozzle, affecting the extrusion start response and quality of the extrudate, leading to failed parts or defects in the part, see figure 2c. A nozzle purging operation is used at the start of each layer which extrudes a small amount of material into a waste bucket, increasing the nozzle back pressure and priming the material flow. Additionally, since the resolution is no longer coupled to the nozzle diameter, a larger diameter (D > 1 mm) nozzle is used to increase throughput and reduce the likelihood of blockages.
- **Dust** – ceramic green machining creates dust from the powdered ceramic. Dust remaining on the machined layer surface causes adhesion issues for subsequent layers. An annular nozzle is installed around the machining spindle that blows air across the tool, cooling the tip and blowing the dust away from the part. However, the dust particles can remain airborne if the particle size is small, creating a respiratory hazard, especially with harmful/toxic ceramic powders. The CHAMP is contained inside an interlocked enclosure with a dust extraction system and HEPA filter.

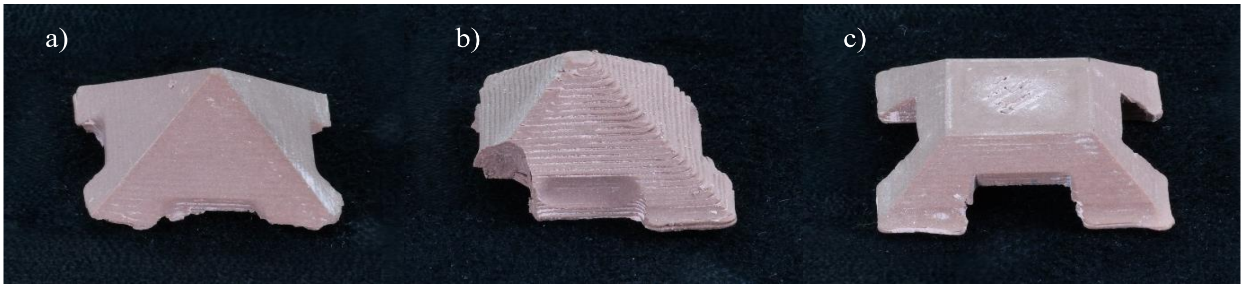

Figure 2 shows examples of failed prints using the CHAMP. Figure 2a) fractured during removal from the build plate, 2b) detached from the build plate during machining operations, 2a) print failed due to nozzle blockage.

- **Defects** – additive manufacturing is prone to systematic and stochastic defects that can detriment the part quality [11]. In-situ monitoring can assist in the operator's analysis of print quality, helping to instruct parameter adjustment for next iteration. Furthermore, the combination of hybrid (AM + SM) manufacturing, process monitoring, and sophisticated control architecture could enable defect-free manufacturing via automated defect correction.

2.2. Process Control

A block diagram of the machine control architecture is shown in figure 4a. The CHAMP is connected to a software motion controller (Mach4, Newfangled Solutions) via EtherCAT fieldbus (750-354, WAGO). The motion controller loads an input GCODE file containing instructions to create the part. Toolpath operations such as printing and machining are controlled directly, assistive operations such as inter-layer drying, and process monitoring, are controlled using custom macros that are stored within Mach4. An outline of the process flow to create a part using the CHAMP is presented in figure 4b.

Typically, GCODE for a specific machine is created using standard slicing software (e.g. Cura, Slic3r etc). However, since the CHAMP is a bespoke platform, no such software exists and a custom pipeline was developed, illustrated as a flowchart in figure 4c. The part was designed, and subtractive toolpaths were generated, using CAD/CAM software (Fusion, Autodesk). The part geometry was exported as an STL file and uploaded into slicing software (Superslicer, Supermerill), which was chosen for its high degree of GCODE customisation. For example, custom macros with height-dependent input variables, such as those for the in-situ monitoring operations, are inserted using the custom GCODEs section. It is also important that the part origin is maintained in the translation between software to ensure toolpath alignment. The additive GCODE was then imported to a python script along with the subtractive toolpaths. The python script compiles the additive and subtractive toolpaths and inserts auxiliary commands such as the start/stop of the auger screw extruder. The hybrid GCODE is then exported and loaded into Mach4 for printing. An example part geometry and corresponding additive GCODE and subtractive toolpaths are shown in figure 3.

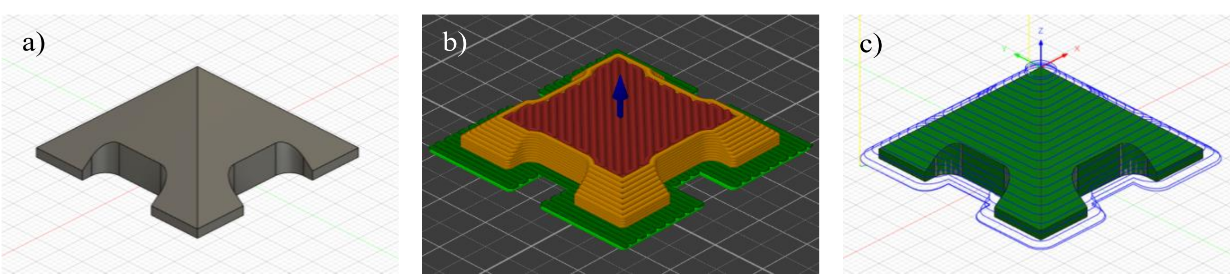

Figure 3a) shows the CAD design of a pyramid demonstrator from Fusion, 3b) shows a visualisation of the additive GCODE midway through the print where green represents the sacrificial raft, yellow is the perimeter, and red is infill (100% density), captured from SuperSlicer, 3c) shows the subtractive toolpath, generated with Fusion.

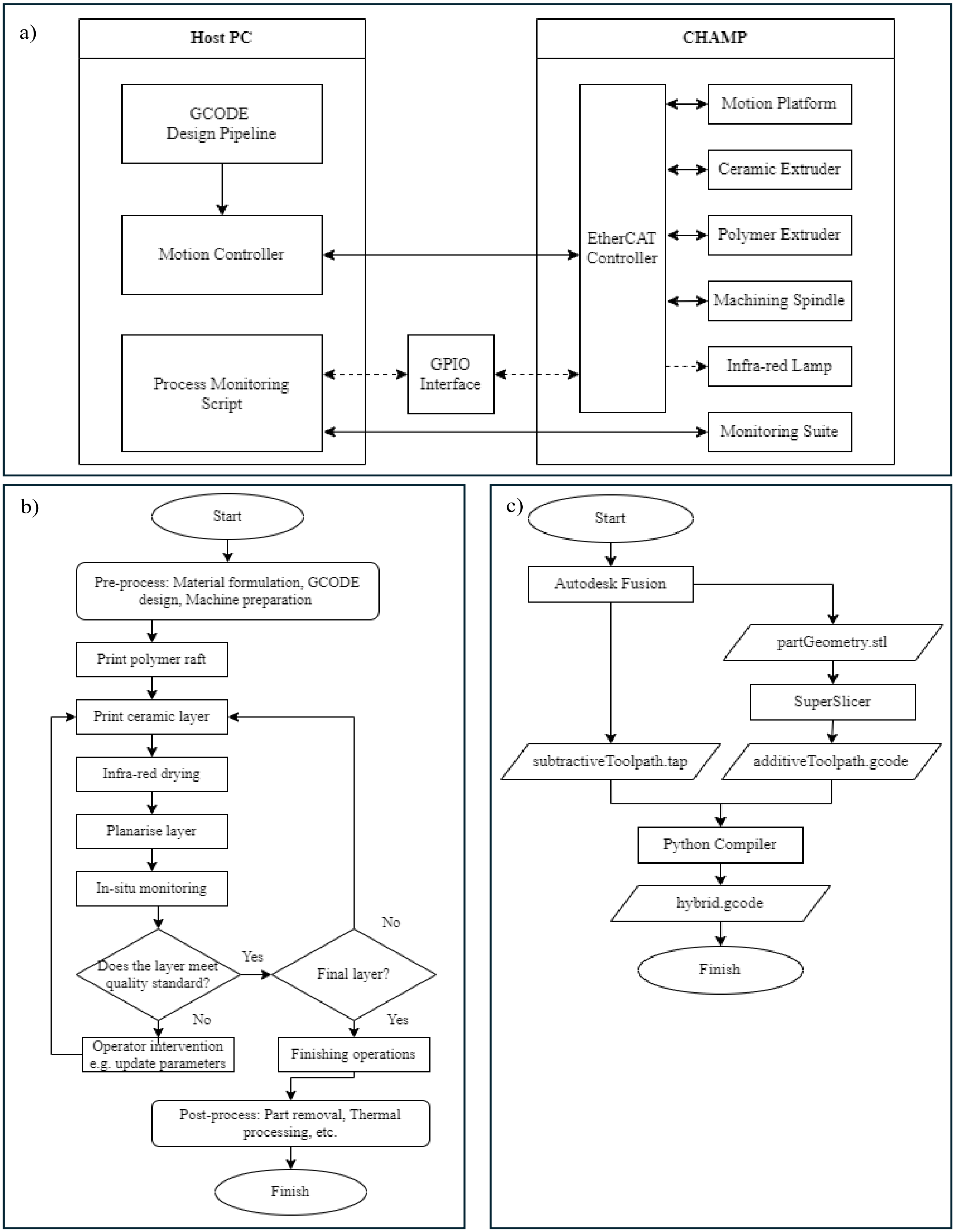

Figure 4c) a block diagram showing the machine control architecture where solid and dashed arrows represent the transfer of data and signal, respectively, 4b) typical process flow for operation of the CHAMP, 4c) the GCODE design pipeline to create hybrid GCODE for the CHAMP.

2.3. Hybrid Manufacturing Strategy

The quality of parts fabricated using the hybrid process depends heavily upon the base process, ceramic paste extrusion. As such, the accuracy and consistency of the extrusion flow rate is critical; paste extrusion is a volumetric process, the exact amount of material should be deposited in a layer of given dimensions. Deviation from the exact volume deposition causes fabrication defects. Figure 5 shows example defects causing by under and overfilling, such as voids which would affect the sintered material properties. The presence of voids (figure 5a) also decreases the strength of the green part and causes fracture or build plate detachment during subsequent machining operations, as shown in figure 2b. Additionally, removal of water content by interlayer drying causes shrinkage of printed material, tending to cause underfilling. Therefore, since the final dimensions are determined by the finishing machining operations, overfilling is beneficial in this process as it precludes void formation. However, excessive overfilling (figure 5b) causes material to build up around the nozzle which can drop onto the printed surface and cause defects in the following layer. Therefore, the current hybrid manufacturing strategy is to deposit an excess of material (extrusion multiplier > 1.1) and planarise each layer at the intended surface height (figure 5c) to avoid cumulative overextrusion effects.

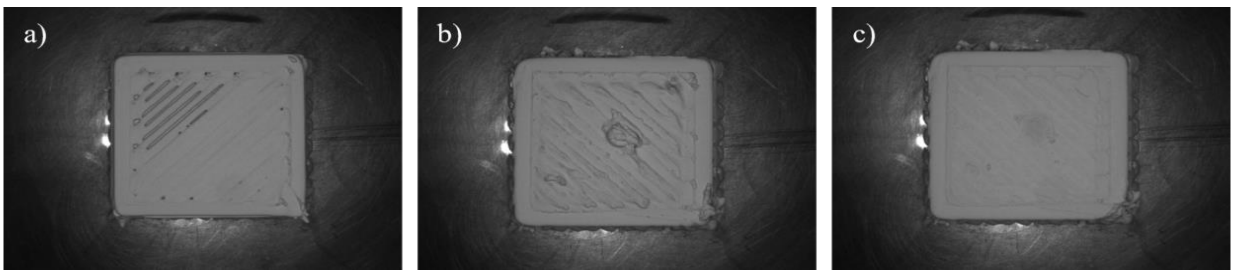

Figure 5a) shows an underfilled layer with voids present, 5b) shows the surface of a printed layer with significant overfilling, 5c) shows the same layer after planarization.

2.4. Sensing

Multi-modal sensing is used in the CHAMP to assess the extrusion quality in-situ. The in-situ measurement suite includes a camera (VCXU.2-201M.R, Baumer Vision Technologies) in a top-down configuration, and a strip laser profilometer (scanCONTROL 2900-50, MicroEpsilon). The measurement is controlled using a process monitoring python script which communicates with the machine via a GPIO hardware link as Mach4 does not natively support a software interface (see figure 4a). The process monitoring script runs an infinite loop, checking each iteration for input signals from Mach4. Each GPIO input triggers a different function. For example, during operation of the camera, a macro is run from GCODE which moves to position and sends a signal to the process monitoring script, activating the camera. Example images of over and under filling defects are shown in figure 5. The images can be used by the operator to help tune extrusion parameters, such as the speed of the auger screw. Additionally, a series of layerwise images is a useful indicator of part quality, which could assist in component certification in regulated industries. Additionally, a large dataset of images could be used to train deep learning models for automated defect detection/correction purposes.

Additionally, the laser profilometer was used to measure part height or detect volume changes of a printed layer during drying, for example. The laser macro moves into position and sends a signal to the monitoring script. It moves across the part surface and scans every 0.5 mm. A second signal is sent to the monitoring script which compiles and performs analysis on the height data, calculating the standard deviation and the modal height. The modal height change during drying was used to calibrate the extrusion flow rate multiplier, compensating for drying shrinkage. However, changes in layer height, layer geometry, and distance to heated build plate during a print suggest that a dynamic approach would be more accurate. However, the lack of data transfer between these software (see figure 4a) limits the ability of this platform to perform intelligent closed loop control, and the use of collected data is currently limited to process analysis and calibration. To realise closed loop control, a direct data link or software interface between the motion controller and the process monitoring script (currently missing) is essential. Development of sophisticated architecture with multi-modal sensing for closed loop control is the subject of ongoing study.

3. Methods

A range of parts were fabricated using the CHAMP to validate the ability of the platform and process to create parts in arbitrary geometries with a range of component and feature sizes. These parts were created to develop an understanding around the effect of different processing parameters and the processes integration. The parts were printed using an aqueous paste material, based on Aluminium Oxide, containing a cellulose-based binder and an electro-steric dispersant. The water content was adjusted to ~27% by weight to enable consistent extrusion but the formulation was not optimised to prevent slumping. Sintering aids (Manganese Dioxide and Titanium Dioxide) were included to reduce the sintering temperature by liquid phase sintering, as recommended by Gnanasagaran *et al.* [12]. Parts were debound for 1 hr at 300 ^{o}C and 1 hr at 500 ^{o}C before sintering for 2 hr at 1500 ^{o}C.

Cubes, with intended sintered dimensions of 20 x 20 x 20 mm, were fabricated to assess the dimensional accuracy, density, and surface roughness of parts made using the hybrid process. Two calibration cubes were used to determine the sintering shrinkage. A third cube was made using this shrinkage compensation. The sintering shrinkage used for the initial cubes was assumed to be 20% based on historic data. The cubes dimensions were captured using the laser profilometer, a non-contact measurement technique, because the parts are fragile in the green state. The mass of the sintered cubes was measured using a microbalance (Practum224-1S, Sartorius Lab Instruments) and the bulk density was calculated using the assumption that the parts were cubic. The surface finish of all three cubes was measured using a contact touch probe (Talysurf Pro, Taylor Hobson). Measurements were taken for the top surface and the side of each cube. Three, 8 mm long, traces were taken per surface at a speed of 0.5, one across the middle and one at each side. A Gaussian filter at 100:1 (8 μm) and LS levelling was applied. The surface roughness of non-machined samples was also measured for comparison against parts produced using a standalone AM process.

4. Results and Discussion

Geometrical Freedom

An image of sample parts produced using the hybrid process is shown in Figure 6. Part g) highlights the improvement in surface finish when the hybrid process is used (left side of hemisphere) compared to the standalone additive process (right side of hemisphere). Part c) shows the pyramid from the earlier GCODE example. Parts b) and f) show the ability of the hybrid method to produce arbitrary complex geometry with curved but smooth surfaces. Part a) shows a minimum wall thickness of 1 mm (~0.8 mm after sintering) could be machined from the green state ceramic. The final wall (0.5 mm) fractured under the load during machining. Slots with thicknesses down to 1 mm were machined into part h) and fine features in complex geometry are shown in parts e) and i). An example cube for measurements of dimensional accuracy, density, and surface roughness is shown in part d).

Dimensional Accuracy

The sintering shrinkage of the two calibration cubes was calculated (relative to the sintered dimension) as ~23 % and ~24 % in the XY and Z directions, respectively. The anisotropic shrinkage is likely to be a result of the layered approach. These shrinkages were used to scale the dimensions of cube 3 in CAD/CAM prior to production. The sintered dimensions of cube 3 were measured as 19.87 x 19.88 x 19.90 mm, giving a maximum dimensional error of 0.13 mm. This suggests a manufacturing resolution of ± 0.13 mm. This is within range of other manual machining operations and high for

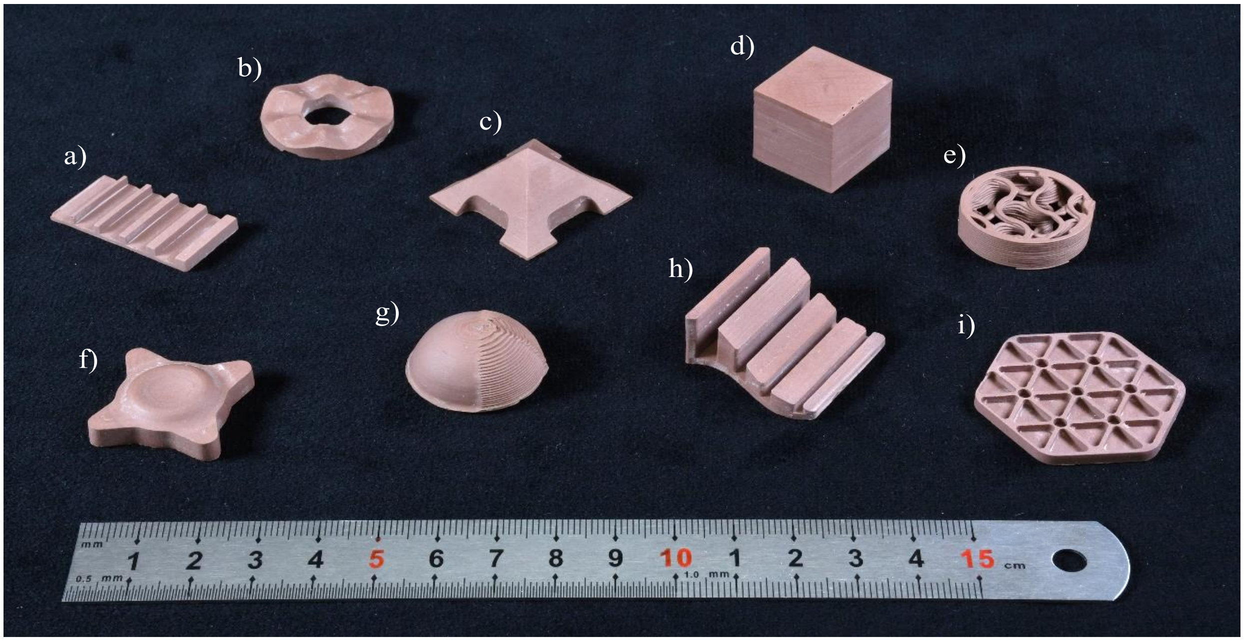

Figure 6 shows sample ceramic components made using the hybrid process. Parts include a) wall thickness test, b) sinusoidal torus, c) quadrupedal pyramid, d) cube, e) gyroid, f) star, g) hemisphere, h) slot milling test, i) isogrid.

ceramic AM, especially once sintering shrinkage is considered. Other studies using ceramic extrusion processes report dimensional accuracies from 0.3 to 1.5 mm [13,14].

Density

The average bulk density of the 3 cubes was calculated as 3.69 g/cm^3. This is comparable to the density of bulk alumina, at 3.99 g/cm^3. This gives a relative density of 92.5 %. The difference is likely due to a combination of residual porosity resulting from organic burnout and fabrication porosity. For example, analysis of the camera data from these parts shows that small voids between perimeter and infill were common during the fabrication of the cubes, see figure 7. To correct this defect, the operator would increase the extrusion multiplier or other toolpath parameters for the next iteration print. To reduce residual porosity, the operator would tune the material formulation/preparation parameters and/or the thermal processing regime.

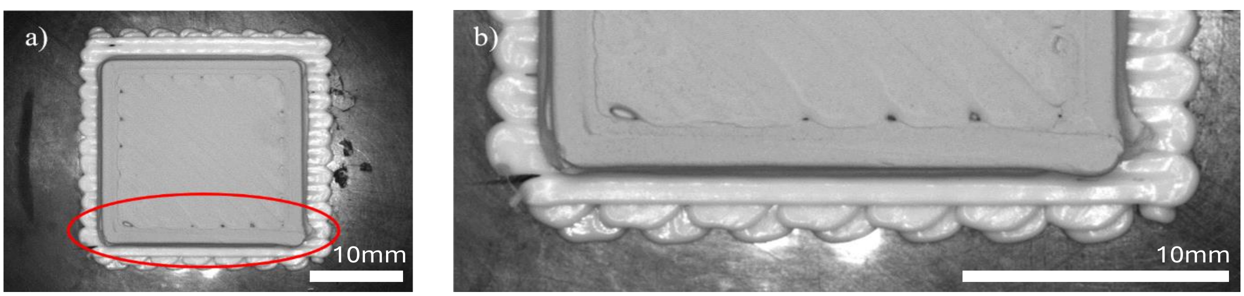

Figure 7a) shows an example layer from cube 3 showing voids between perimeter and infill due to underfilling, 7b) shows a close-up view of the region circled in red.

Surface Roughness

The surface roughness; Ra, of non-machined samples were measured at 5.35 µm and 27.81 µm for the top and side surfaces, respectively. The roughness of the non-machined side surface is high due to the presence of layer lines, a common feature of parts produced using additive (layered) manufacturing techniques; paste extrusion literature reports surface roughness values between 25 and

45 μm [14]. The texture of the non-machined top surface is due to the superposition of distinct extrusion widths when overfilling. The Ra of the machined cubes was measured at an average of 1.96 μm and 1.83 μm for the top and side surfaces of the cubes, respectively. This is representative of approximately 3x and ~15x improvement in surface finish by the sequential operation of green machining operations within the hybrid-AM process. This could be further improved by fine tuning the cutting parameters.

5. Conclusion

A hybrid-AM method was developed to overcome limitations of the standalone manufacturing processes. This involved the development of a ceramic hybrid additive manufacturing platform (CHAMP) and a corresponding software package for process control (GCODE design) and sensor integration. While the specifics of this software package are machine specific, the methodology could be applied to alternative hybrid-AM platform for research and development purposes.

The hybrid method involved the extrusion of a sacrificial, polymeric support material for improved handleability, followed by a loaded ceramic paste material, without optimised rheology. The paste was dried layer-by-layer using an infra-red lamp, developing a yield stress to avoid slumping and enable green machining operations. Machining operations are then used for layerwise planarisation and finishing operations, improving the dimensional accuracy and surface finish. Several demonstrators were fabricated, demonstrating the novel capability of the hybrid platform, process, and software to produce parts in a range of arbitrary, complex geometries. A dimensional accuracy of ± 0.13 mm and a surface finish of less than 2 μm were achieved for cubic samples with relative density of 92.5 %. Comparing these values to literature verifies the ability of the hybrid method to fabricate ceramic components with improved quality over an equivalent standalone AM process.

The use of sensing for closed loop control was limited in the current platform by the lack of software integration (motion control + process monitoring). However, sensing was used to analyse print quality and instruct parameter optimisation, improving part quality. A control architecture was proposed that would enable autonomous closed-loop parameter optimisation and defect correction which will be the subject of ongoing study.

7. References

[1] M.P. Sealy, G. Madireddy, R.E. Williams, P. Rao, M. Toursangsaraki, Hybrid processes in additive manufacturing, Journal of Manufacturing Science and Engineering, Transactions of the ASME 140 (2018). https://doi.org/10.1115/1.4038644.

[2] J. Hinton, D. Basu, M. Mirgkizoudi, D. Flynn, R. Harris, R. Kay, Hybrid additive manufacturing of precision engineered ceramic components, Rapid Prototyping Journal 25 (2019).

[3] D.A.J. Brion, S.W. Pattinson, Generalisable 3D printing error detection and correction via multi-head neural networks, Nat Commun 13 (2022). https://doi.org/10.1038/s41467-022-31985-y.

[4] N. Travitzky, A. Bonet, B. Dermeik, T. Fey, I. Filbert-Demut, L. Schlier, T. Schlordt, P. Greil, Additive Manufacturing of Ceramic-Based Materials, Adv Eng Mater 16 (2014) 729–754. https://doi.org/10.1002/ADEM.201400097.

[5] J. Deckers, J. Vleugels, J.P. Kruth, Additive manufacturing of ceramics: A review, Journal of Ceramic Science and Technology 5 (2014) 245–260. https://doi.org/10.4416/JCST2014-00032.

[6] W. Li, A. Ghazanfari, M.C. Leu, R.G. Landers, Extrusion-on-demand methods for high solids loading ceramic paste in freeform extrusion fabrication, Virtual and Physical Prototyping (2017). https://doi.org/10.1080/17452759.2017.1312735.

[7] M.S. Mason, T. Huang, R.G. Landers, M.C. Leu, G.E. Hilmas, Aqueous-based extrusion of high solids loading ceramic pastes: Process modeling and control, J Mater Process Technol 209 (2009) 2946–2957. https://doi.org/10.1016/J.JMATPROTEC.2008.07.004.

[8] Y. Lakhdar, C. Tuck, J. Binner, A. Terry, R. Goodridge, Additive manufacturing of advanced ceramic materials, Prog Mater Sci 116 (2021) 100736. https://doi.org/10.1016/J.PMATSCI.2020.100736.

[9] J.E. Smay, J. Cesarano, J.A. Lewis, Colloidal Inks for Directed Assembly of 3-D Periodic Structures, Langmuir 18 (2002) 5429–5437. https://doi.org/10.1021/LA0257135.

[10] J.S. Reed, Introduction to the principles of ceramic processing, Wiley, 1988.

[11] A.L. Petsiuk, J.M. Pearce, Open Source Computer Vision-based Layer-wise 3D Printing Analysis, n.d.

[12] C.L. Gnanasagaran, K. Ramachandran, S. Ramesh, S. Ubenthiran, N.H. Jamadon, Effect of co-doping manganese oxide and titania on sintering behaviour and mechanical properties of alumina, Ceram Int 49 (2023) 5110–5118. https://doi.org/10.1016/J.CERAMINT.2022.10.027.

[13] F. Hu, T. Mikolajczyk, D.Y. Pimenov, M.K. Gupta, Extrusion-based 3d printing of ceramic pastes: Mathematical modeling and in situ shaping retention approach, Materials 14 (2021) 1–22. https://doi.org/10.3390/MA14051137.

[14] I. Buj-Corral, A. Domínguez-Fernández, A. Gómez-Gejo, Effect of printing parameters on dimensional error and surface roughness obtained in direct ink writing (DIW) processes, Materials 13 (2020). https://doi.org/10.3390/ma13092157.